JOURNAL OF ENERGY SYSTEMS

VOLUME 3, ISSUE 3

2602-2052

DOI: 10.30521/jes.605085

Research Article

Spray deposited thin films of SnO_2: F/CdS: In bilayers produced using different fluorine sources: NH_4F and HF

Shadia J. Ikhmayies

Isra University, Faculty of Science, Department of Physics, Amman, Jordan, shadia_ikhmayies@yahoo.com

Arrived: 11.08.2019 Accepted: 31.08.2019 Published: 30.09.2019

Check for Updates

Abstract: Thin films SnO_2: F/CdS: In bilayers were prepared using the spray pyrolysis method on glass substrates at a substrate temperature T_s = 450 °C. Ammonium fluoride (NH_4F) and hydrofluoric acid (HF) were both used as the fluorine sources in the precursor solution of SnO_2: F. Properties of the two types of bilayers obtained using the two fluorine sources were investigated. X-ray diffraction (XRD), scanning electron microscopy (SEM) and transmittance measurements (UV-Vis) were used to characterize the films. It is found that the bilayers prepared using HF as a source of fluorine have more ordered crystal growth, and sharper absorption edge. From the inspection of the first derivative of the absorbance it is expected that more interdiffusion on the SnO_2: F/CdS: In interface takes place in the bilayers produced using HF. These results confirm that these bilayers are better as fore contacts for thin film CdS/CdTe solar cells.

Keywords: *Spray pyrolysis, Thin films, CdS/CdTe thin film solar cells, Transparent conducting oxides, Cadmium compounds.*

Cite this paper as: *Ikhmayies, S.J., Spray deposited thin films of SnO2: F/CdS: In bilayers produced using different fluorine sources: NH4F and HF, Journal of Energy Systems 3(3);(2019); 111-122, DOI: 10.30521/jes. 605085*

1. INTRODUCTION

Thin film CdTe/CdS polycrystalline solar cells are of the most suitable photovoltaics because they are cheap, stable, and provide large area [1]. When they are built in the superstrate geometry [2,3] they rely on transparent conducting oxides (TCOs) to make the front contact. But the ideal front contact for the solar cell must have low resistivity and high transparency. In addition, it must be chemically stable in subsequent processing steps, and there is no energy barrier for charge transport [4]. The investigation of combined CdS/TCO bilayer films has recently been developed due to the importance of better understanding the effect of these bilayers on the absorbers [5,6]. In most cases, tin oxide (SnO_2) is utilized as the front contact for this type of solar cells, where best energy conversion efficiencies have been obtained with SnO2 contacts so far [4]. Hence, optimizing the properties of the SnO_2/CdS structures is an important step on the way to get high performance CdS/CdTe solar cells.

There are different experimental routs to prepare SnO_2 thin films, such as reactive sputtering [7], thermal evaporation [8-10], chemical vapor deposition [8,11], dip coating [12] and spray pyrolysis [13-25]. At the same time CdS thin films can be prepared by different methods such as chemical bath deposition [26], thermal evaporation [27-29], screen printing [30] and spray pyrolysis [14,28,31-45]. However, the spray pyrolysis method is a low cost and simple method, which enables intentional doping, and getting large area, and uniform thin films [46]. For these reasons it is chosen to produce both SnO_2 and CdS layers in this work. To improve the properties of these compound semiconductors, SnO_2 was doped with fluorine, and CdS was doped with indium, where such doping is well known for these compounds.

Few research was conducted on investigating the SnO_2/CdS structures, because CdS/CdTe interface had attracted attention. The CdS/TCO bilayer allows collecting the carriers, the highly conductive and transparent TCO film being used to avoid large loss of energy, which could be induced by the highly resistive CdS layer. Therefore, in order to optimize the performance of the solar cell, more understanding of the grain morphology and interface properties is very important for optimal electrical, optical and junction properties [47]. Niles et al. [48] had investigated the formation and thermal stability of the SnO_2/CdS interface by soft X-ray synchrotron radiation photoemission. Krishnakumar et al. [49] had investigated the band alignment of differently treated TCO/CdS interface, where they found the band offset at differently prepared and treated ITO/CdS and SnO_2/CdS interfaces using photoelectron spectroscopy, and sputter depth profiling, Al Turkestani and Durose [50] studied rectification in CdS/TCO bilayers, and we [6] studied the characteristics of SnO_2: F/CdS: In structures prepared by the spray pyrolysis technique. Fritsche et al. [4] have investigated the properties of the CdS/SnO2 interface by X–ray and ultraviolet photoelectron spectroscopy.

The objective of this work is to investigate the influence of different dopant of the SnO_2 layer on the properties of the SnO_2; F/CdS; in bilayer. The SnO_2: F/CdS: In bilayers were produced using the spray pyrolysis method, but two different doping compounds NH_4F and HF were used as sources of fluorine to prepare the SnO_2: F precursor solution. The CdS: In was deposited onto SnO_2: F samples prepared using both of NH_4F and HF. It is found that different structural, morphological, and optical properties for samples of different fluorine sources. These results are consistent with the results found in references [18,25,51], where considerable differences were observed in the properties of the films obtained using NH_4F and HF as sources of fluorine in the SnO_2: F precursor solution, and it is found that bilayers produced by using HF are better for the production of CdS/CdTe solar cell than those produced using NH_4F.

2. METHODOLOGY

Stannous chloride $SnCl_2.2H_2O$ was used to prepare the precursor solution for SnO_2:F thin films. The sources of fluorine used are ammonium fluoride NH_4F (BDH Chemicals. Ltd Poole England), and hydrofluoric acid HF (40%). Two different solutions were prepared: The first solution was prepared from 5.03×10^{-3} moles of stannous chloride ($SnCl_2.2H_2O$), and 4.73×10^{-3} moles of ammonium fluoride (NH_4F). These were dissolved in 45 ml of methanol CH_3OH (MAY AND BAKER LTD DAGENHAM ENGLAND), 5 ml of distilled water, and 1 ml of HCl. The ratio of fluorine ions to tin ions in the solution was 0.94 which is approximately the same as that used by Gordillo et al. [15] at which they got the best quality of SnO_2: F films prepared by using NH_4F. This solution was sprayed onto glass substrates of dimensions $2.5\times6\times0.1$ cm^3 that were ultrasonically cleaned in methanol at substrate temperature T_s = 450 °C for at least 15 minutes. The set of bilayers prepared from this solution is called NH_4F-films. The second solution was made by dissolving 5.01×10^{-3} moles of $SnCl_2.2H_2O$ with 5.71×10^{-3} moles of HF in 45 ml of methanol, 5 ml of distilled water and 1 ml of HCl. The ratio of fluorine ions to tin ions in the solution was 1.14 which is also approximately the same as that used by Gordillo et al. [15] at which they got the best SnO_2: F films prepared by using HF. This solution was sprayed on ultrasonically cleaned glass substrates similar to those used above, where the same spraying method and period were used. The set of bilayers prepared from this solution is called HF-films.

The CdS: In precursor solution was prepared by taking 2.06×10^{-2} moles of extra pure $CdCl_2.H_2O$ (MERCK Art. 2011) and 2.24×10^{-2} moles of thiourea $(NH_2)_2CS$ (>97% S) in 350 ml of distilled water. Indium chloride $InCl_3$ (MERCK Art.12471) was used as the source of indium. The ratio of the concentration of indium ions to that of cadmium ions in the solution ($[In^{+3}]/[Cd^{+2}]$) which is approximately the same ratio of the corresponding atoms was 10^{-4}. This ratio differs from that in the films due to the dynamic nature of the spray pyrolysis. In-doped CdS thin films have been deposited onto the NH_4F-films and HF-films prepared before at a substrate temperature T_s = 450 °C. The produced structures are denoted by NH_4F-structures and HF-structures respectively. The spraying system used to produce the films has been described elsewhere [14]. The spray rate was usually in the range 15-18 ml/min. Nitrogen was used as the carrier gas, and the optimum carrier gas pressure for this rate of solution flow was around 5 kg/cm^2.

Structure and phase of the films were analyzed using X-ray diffraction measurements, which are recorded using a Philips Analytical Compact X-ray diffractometer system with cobalt (Co) anode material, where X-ray lines $K_{\alpha1}$ (λ_1 = 1.78897Å) and $K_{\alpha2}$ (λ_2 = 1.79285Å) are used. The surface morphologies of the films are analyzed using a LEITZ-AMR 1000A scanning electron microscope, while composition was determined by Energy Dispersive X-ray analysis (EDX) using FEI Inspect F50. The transmittance of the films was recorded at room temperature in the wavelength range $\lambda = 290 - 1100\,nm$ using a double beam Shimadzu UV 1601 (PC) spectrophotometer with respect to a piece of glass similar to the substrates.

3. RESULTS and DISCUSSION

Figure 1 shows the X-ray diffractograms of two SnO_2: F/CdS: In bilayers deposited at a substrate temperature T_s = 450 ˚C. Figure 1a is for the NH_4F-film, and Figure 1b is for the HF-film, and the thickness of the CdS: In layer is approximately the same (≈ 100 nm) in both bilayers. The diffractograms show the crystallographic orientations of the hexagonal phase of CdS which is referred to as H, but it is not easy to recognize the lines characteristic of SnO_2, which are weaker than those of CdS and sometimes overlapped with them. Diffraction peaks of the cubic phase of CdS referred as C, are not observed too.

But the line C(111) of cubic phase overlaps the line H(002) of the hexagonal phase. CdS diffraction peaks are assigned to the corresponding Miller indices as shown in the figure, where the following peaks are observed H(100), C(111)/H(002), H(101), H(102), H(110), H(103), and H(112). Table 1 lists the XRD data for the two sets of SnO_2:F/CdS: In bilayers, which includes the interplanar spacing d, intensity of the peaks, and Miller indices, where d was measured for the two cobalt anodes (α_1 = 1.78897 Å and α_2 = 1.79285 Å).

The comparison between the two diffractograms shows the differences: First, the orientation of crystal growth is more ordered in Figure 1b. Second, the intensities of the lines H(100), H(102), H(110), H(103) and H(112) in Figure 1b are smaller than their intensities in Figure 1a. Third, the line C(111)/(002) have larger intensity in Figure 1b, and it represents the preferential orientation, while the line (101), which was the preferential orientation in Figure 1a is weaker in Figure 1b. Fourth, the intensity of the peaks of positions $2\theta < 23°$ had too much suppressed in Figure 1b , where these peaks are related to the formation of complex compounds that decompose to CdS [41]. Finally from table 1 it is noticed that the interplanar spacing d is in general larger for the bilayers produced using NH_4F, or in other words for the bilayers prepared using HF, the whole diffractograms was shifted towards smaller d values.

This behavior can be interpreted depending on the results of the compositional analysis obtained using EDX measurements shown in table 2. As seen in table 2, the ratio of oxygen atoms to tin atoms in HF-films is 1.96, which is very close to the stoichiometric ratio 2.0, but in NH_4F-films, it is 8.47, which is very far from the stoichiometric ratio. It is known that the ionic radius of tin ion Sn^{4+} is smaller than that of oxygen ion O^{2-}, so the larger density of oxygen ions and smaller density of tin ions enlarges the lattice and hence lattice parameters, which results in larger interplanar spacing d, which is the case of the NH_4F-films. Despite the fact that more fluorine the NH_4F- films have larger fluorine content -as seen in table 2- but the large ratio of oxygen concentration to tin concentration in these films reduces their quality for the use in CdS/CdTe thin film solar cells.

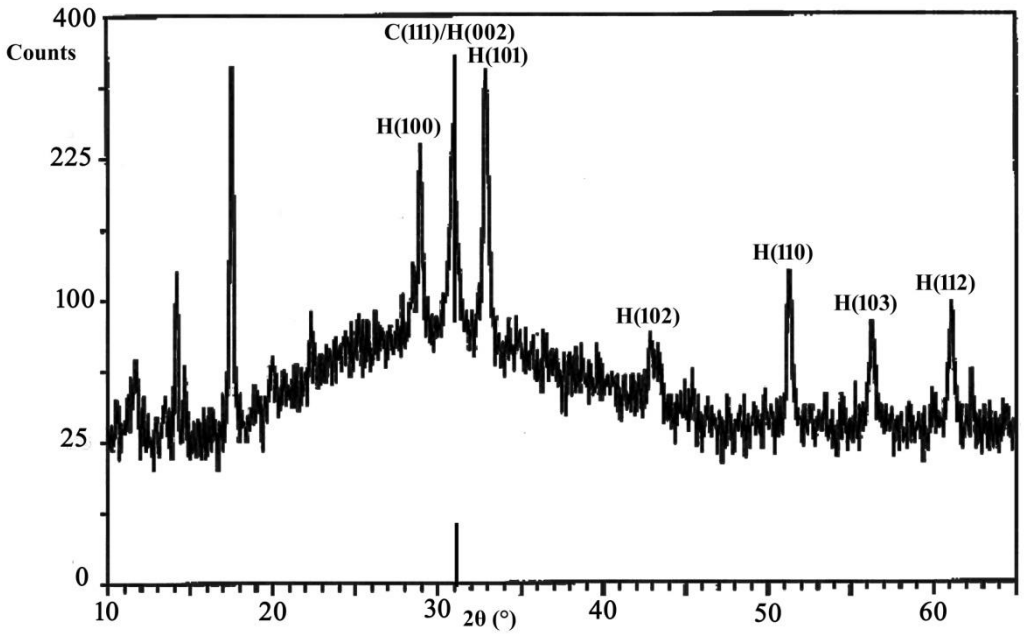

(a)

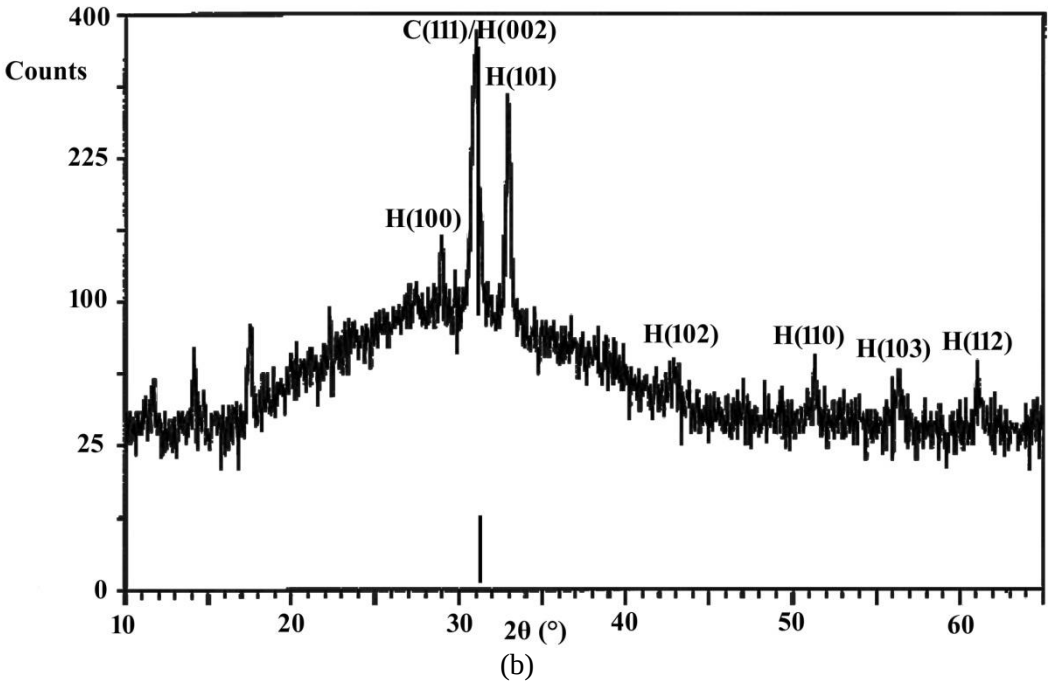

(b)

Figure 1. X-ray diffractograms of SnO_2: F/CdS: In bilayers NH_4F-film (a), and HF-film (b).

Table 1. The XRD data of the SnO_2: F/CdS: In bilayers; NH_4F-film and HF-film.

2θ of the peaks (˚)	d for α_1(Å)	NH_4F-film d for α_2(Å)	(hkl)	Height (Counts)	2θ of the peaks (˚)	d for α_1(Å)	HF-film d for α_2(Å)	(hkl)	Height (Counts)
11.695	8.77967	8.79874		32	11.660	8.80594	8.82506		14
13.390	7.67242	7.68909		14					
14.175	7.24952	7.26527		96	14.185	7.24444	7.26017		19
14.675	7.00381	7.01902		24					
17.560	5.86005	5.87277		313	17.560	5.86005	5.87277		49
19.945	5.16518	5.17640		18					
22.370	4.61127	4.62128		29	22.290	4.62761	4.63766		24
28.950	3.57854	3.58631	H(100)	172	28.975	3.57552	3.58328	H(100)	58
31.005	3.34661	3.35387	H(002)	164	31.010	3.34608	3.35335	H(002)	292
32.930	3.15592	3.16278	H(101)	262	32.940	3.15499	3.16184	H(101)	193
42.790	2.45201	2.45734	H(102)	26	42.850	2.44874	2.45406	H(102)	11
51.260	2.06789	2.07238	H(110)	90	51.325	2.06545	2.06993	H(110)	26
56.320	1.89535	1.89947	H(103)	42	56.370	1.89381	1.89792	H(103)	17
61.110	1.75953	1.76335	H(112)	67	61.065	1.76070	1.76452	H(112)	18

Table 2. The results of the EDX analysis for SnO_2: F/CdS: In bilayers NH_4F-films, and HF-films.

Element	NH_4F Norm.(wt%)	HF Norm.(wt%)
O	88.47±28.4	65.62±21.5
F	1.08±1.3	0.85±1.6
Sn	10.44±5.0	33.52±13.2

The values of the interplanar spacing d can be used to calculate the lattice constants of CdS:In on SnO_2:F substrates prepared using NH_4F and HF as fluorine sources. For hexagonal crystals the following relationship connects d and lattice constants a and c [52];

$$\frac{1}{d_{hkl}^2} = \frac{4(h^2 + hk + k^2)}{3a^2} + \frac{l^2}{c^2} \quad (1)$$

where $h, k,$ and l are Miller indices. A plot of $1/d_{hkl}^2$ against l^2 is performed and shown in Figure 2, where Figure 2a shows the plot for NH_4F-films and Figure 2b shows that for HF-films. The relationships are linear, and data points for the two cobalt anodes α_1 and α_2 coincide with each other. A linear fit is performed for each figure, and fit parameters are shown as insets. From the slopes it is found that the values of c are 6.706 ± 0.011 Å, and 6.698 ± 0.008 Å for NH_4F films and HF-films respectively, and, from the intercept the value of a are $4.136 \pm 9.14 \times 10^{-3}$ Å and $4.133 \pm 6.80 \times 10^{-3}$ Å for NH_4F films and HF-films respectively. These values are smaller than the known values $c = 6.756$ Å and $a = 4.160$ Å [53].

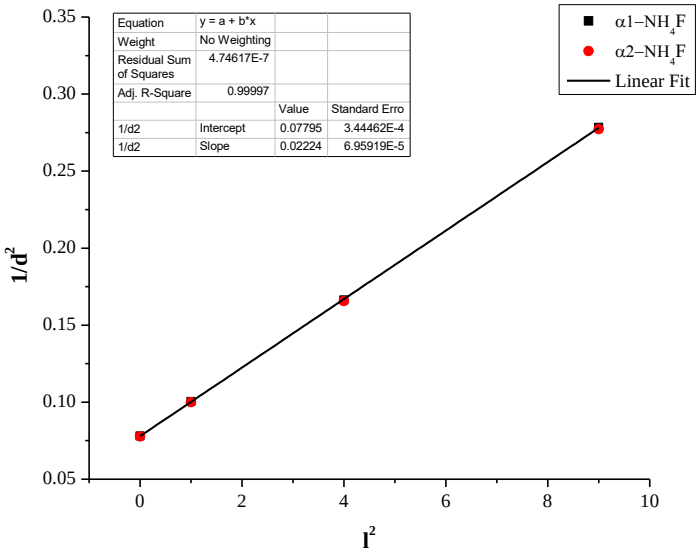

(a)

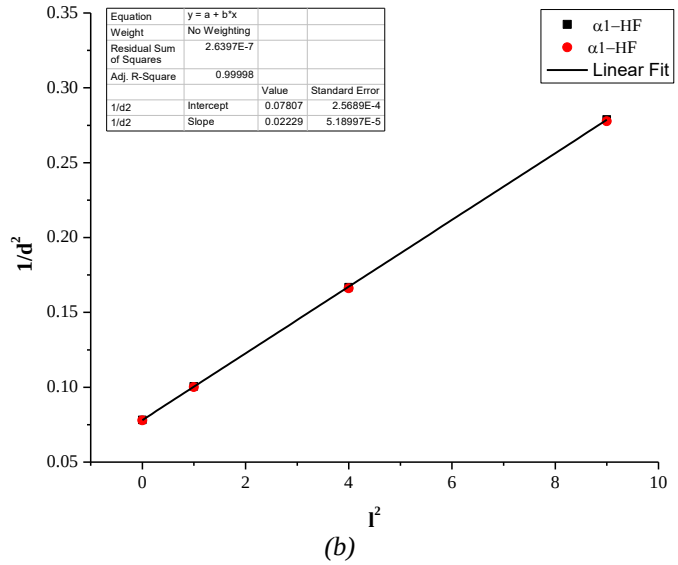

(b)

Figure 2. Plots of $1/d^2$ against l^2 for NH4F-films (a), and HF-films (b).

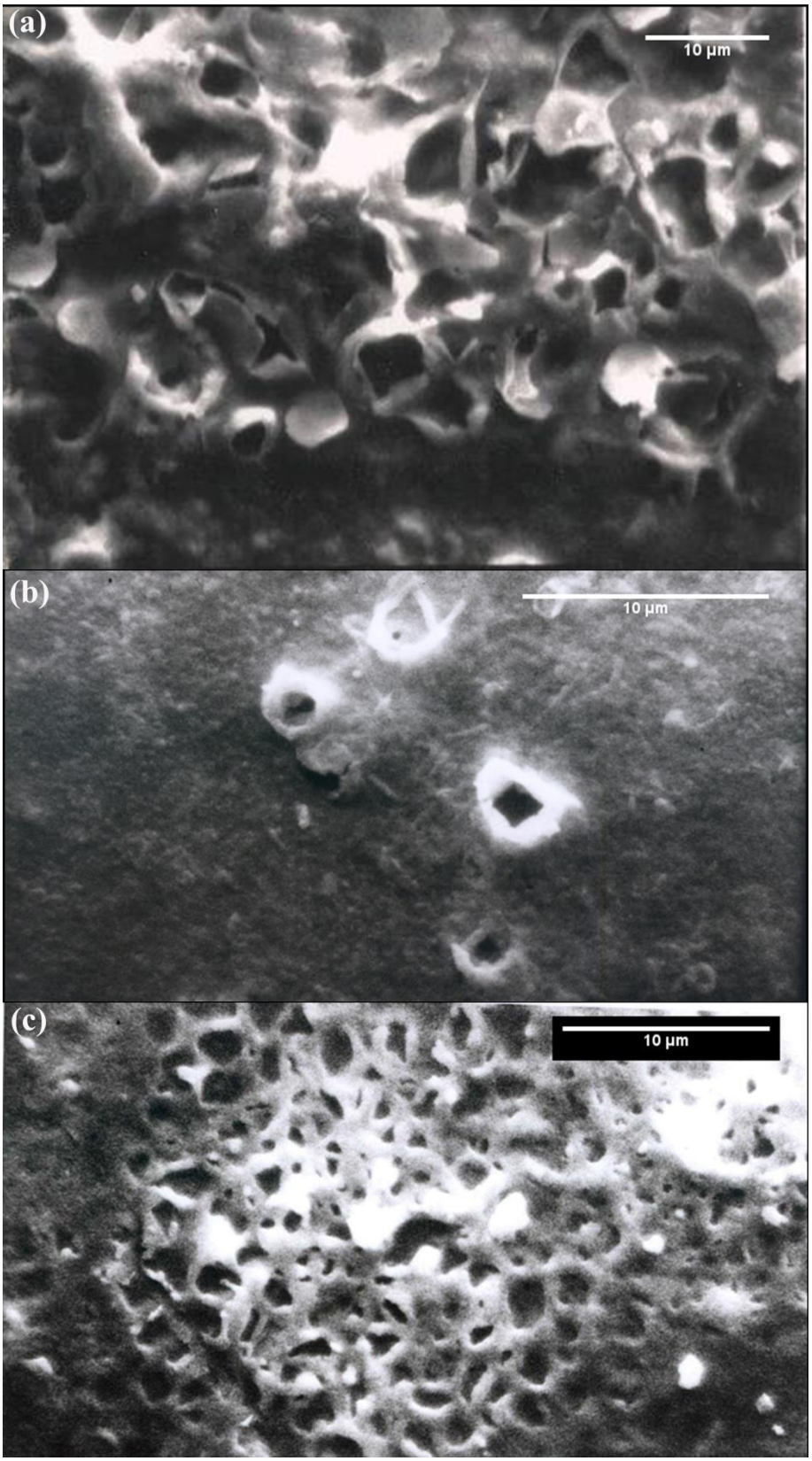

Figure 3. SEM images of: a) CdS: In on glass substrates at T_s = 460 °C [41]. b) SnO_2:F/CdS: NH_4F-films. c) SnO_2:F/CdS: HF-films.

Figure 3 displays the SEM images of CdS: In deposited on three substrates, where Figure 3a shows the SEM of CdS: In on glass, Figure 3b shows the SEM of CdS: In/SnO_2:F named NH_4F-film, and Figure

3c shows that of CdS: In/SnO_2:F named HF-films. The differences in surface morphologies are apparent in the three cases, and the NH_4F-film presents the smallest grain size of the CdS: In layer.

These results confirm that the properties of the films depend on fluorine source or in general on the precursor solution. There is consistence with Dhere et al. [54], who produced SnO_2 films by chemical vapor deposition using tin tetrachloride and tetramethyltin precursors, and found that the preferential orientation and morphology of the films are functions of the precursor used and the growth temperature.

Figure 4 displays the transmittance and absorbance of the two sets of SnO_2: F/CdS bilayers (NH_4F-films and two HF-films), where the measurements were recorded for two films of each set. As Figure 4a shows, all of the films have approximately the same transmittance after $\lambda \geq 510nm$, i.e. after the absorption edge of CdS. This is because the transmittance in this region is determined by the CdS: In layer. But before the absorption edge of CdS ($\lambda < 510\,nm$) there are apparent differences. The transmittance of the NH_4F-films in this region is larger than that of the HF-films. This means that the absorbance of the HF-films is higher in this region. Figure 4b confirms this expectation, where it is obvious that the absorbance of the HF-films is larger than that of the NH_4F-films before the absorption edge of CdS. The higher absorption is due to the larger density of free charge carriers which are electrons in the case of SnO_2: F. From table 2 it is seen that the NH_4F-films are richer in oxygen and poorer in tin than the HF-films. This means that the density of the defects such as O^-, O_2^- and Sn deficiency, is larger in the NH_4F-films.These defects reduce the density of free charge carriers (electrons) in the films. Although the NH_4F-films contain more fluorine than the HF-films, and they have a higher doping ratio, where the doping ratio is the ratio of the concentration of fluorine ions to that of tin ions. That is approximately the same as the ratio of the atoms [F]/[Sn], and it is 2.5% in the HF-films and 10.34% in the NH_4F-films, but the ratio of the concentration of fluorine ions to that of oxygen ions which is approximately the same as that of the atoms is 13% for the HF-films, but 1.22% for the NH_4F-films. It is expected that fluorine replaces oxygen in the SnO_2 lattice, and hence it increases the density of free electrons.

Figure 5 displays the first derivative of the absorbance against wavelength. The minima in the graph refer to the band gap value. At least two minima are observed in the graph, one for CdS: In and the other for SnO_2:F. The minima at about 500 nm refer to the bandgap of CdS: In which is about 2.48 eV. As the figure shows the positions of these minima are approximately the same for both sets of films. But it is obvious that the minima are deeper in the case of the HF-films, which means that the absorption edge is sharper. The other minima refer to the bandgap of SnO_2: F which is about 4.17 eV. Also all of the films showed approximately the same positions of the minima. In addition, the minima are deeper, and wider in the case of the HF- films. The width of the minima could be due to the distribution in the grain size, where each size results in a certain minimum and the superposition of these minima produces the wide minimum that we have. Minima can be related to interdiffusion on the junction and the formation of a solid solution of the form CdS_xSn_{1-x}.

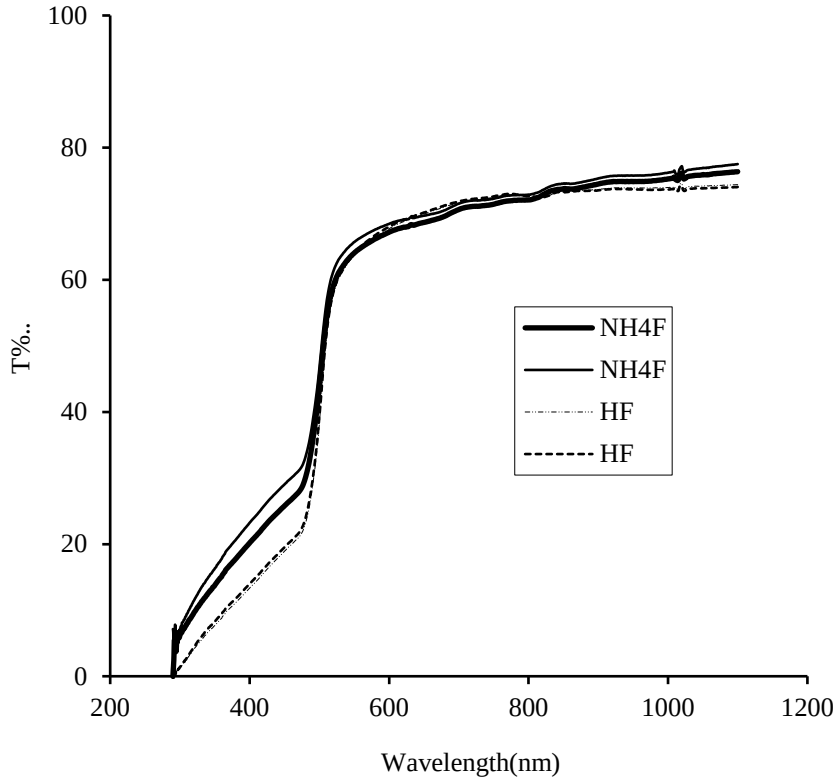

(a)

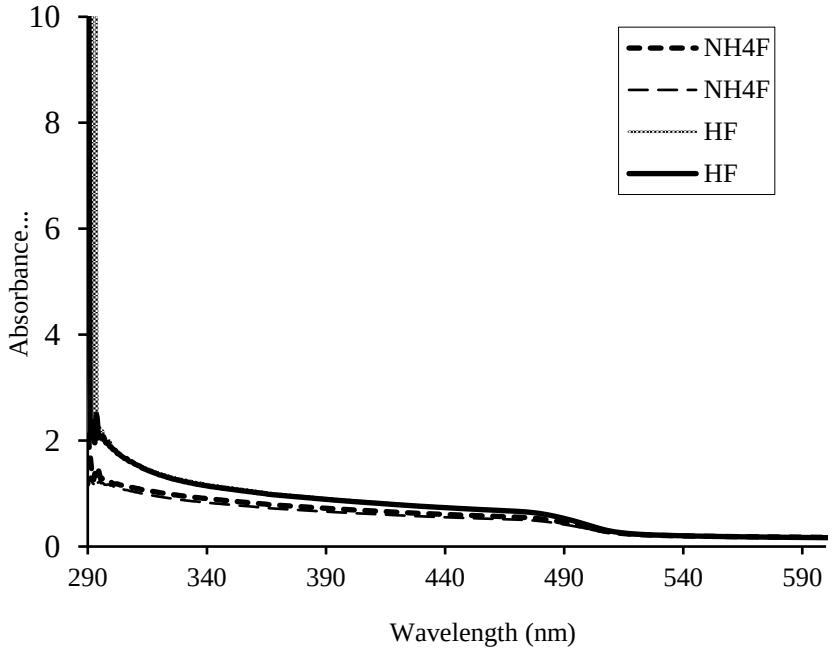

(b)

Figure 4. a) The transmittance curves of the SnO_2: F/CdS: bilayers. b) The absorbance curves of the SnO_2: F/CdS: In bilayers.

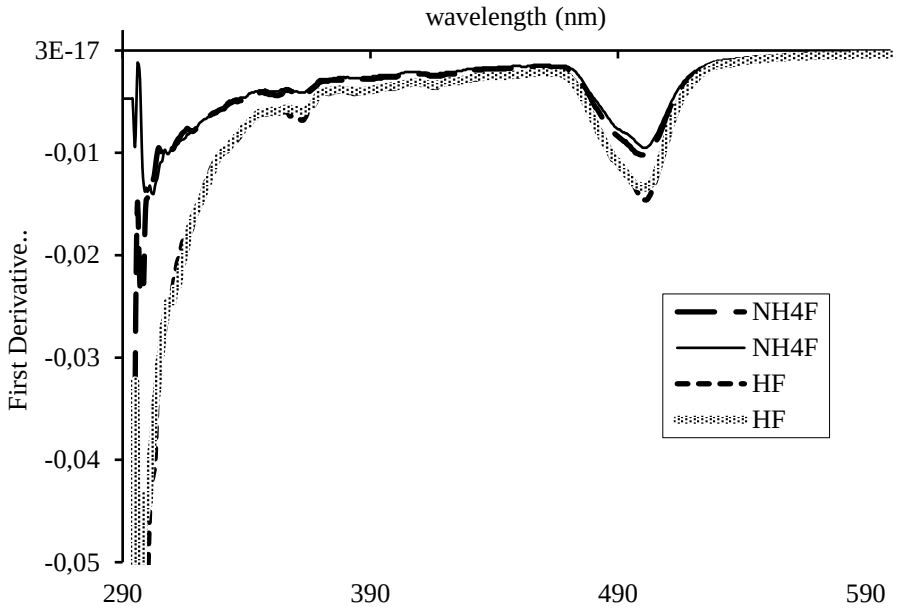

Figure 5. The plot of the first derivative of the absorbance against the photon's energy of the SnO_2: F/CdS: bilayers.

4. CONLUSIONS

Thin films of SnO_2: F/CdS: In bilayers were prepared using the spray pyrolysis method by both NH_4F and HF as sources of fluorine, where each one is separately used. XRD diffractograms revealed the hexagonal phase of CdS and that the HF-films have more ordered crystal growth and larger grain size than the NH_4F-films. SEM observations showed different morphologies and larger grain size for the HF-films. EDX analysis revealed that the NH_4F- films are richer in oxygen and poorer in tin, which reduces the density of free charge carriers. The transmittance of the HF- films is smaller in the high energy region before the absorption edge of CdS due to stronger absorption. From the first derivative curves, it is found that the bandgap energies of CdS: In and SnO_2:F did not change, but the wide minima of SnO_2:F may refer to interdiffusion on the SnO_2:F side. The deeper minima in the case of HF-films refer to sharper absorption edge. From these results it is found that HF is a better fluorine source in the SnO_2: F layer to be used as a fore contact in superstrate CdS/CdTe solar cells.

REFERENCES

[1] Kariper, A, Güneri, E, Göde F, Gümüş, C, Özpozan, T. The structural, electrical and optical properties of CdS thin films as a function of pH. *Materials Chemistry and Physics, 2011; 129*: 183- 188.

[2] Aissat, A, Arbouz, H, Vilcot, PJ. Modeling and optimization of a superstrate solar cell based on $Cu_2ZnSn(S_xSe_{1-x})_4$/ZnS structure. *Journal of Energy Systems, 2017; 1*(2): 65-74 DOI: 10.30521/jes.349137

[3] Ikhmayies, SJ. Properties of the CdS_xTe_{1-x} solid solution: As a single product and as a part of the CdS/CdTe solar cell. *Journal of Energy Systems, 2017, 1*(3): 102-110 DOI: 10.30521/jes.355507

[4] Fritsche, J, Gunst, S, Thissen, A, Gegenwart, R, Klein, A, Jaegermann, W. CdTe thin film solar cells: The CdS/SnO_2 front contact, *Mat. Res. Soc. Symp. Proc., 2001*; 668: H5.1.1- H5.1.6. DOI: 10.1557/PROC-668-H5.1
[5] Martínez, MA, Guillén, C, Gutiérrez, MT, Herrero, J. Optimisation of CdS-TCO bilayers for their application as windows in photovoltaic solar cells. *Solar Energy Materials and Solar Cells, 1996; 43:* 297-310.
[6] Ikhmayies, SJ, Ahmad-Bitar RN. Characterization of the SnO_2: F/CdS: In structures prepared by the spray pyrolysis technique. *Solar Energy Materials and Solar Cells, 2010; 94*: 878-883.
[7] Pan, SS, Ye, C, Teng, XM, Fan, HT, Li, GH. Preparation and characterization of nitrogen-incorporated SnO_2 Films. *Appl Phys. A, 2006; 85*(1): 21-24.
[8] Montmeat, P. Thin film membranes for the improvement of gas sensor selectivity, *Doctorate thesis. École Nationale Supérieure des Mines de Saint-Étienne (ENSMSE): a graduate school for science and technology*, Saint-Étienne, France, 1999.
[9] Ikhmayies, SJ. Properties of amorphous SnO_2 thin films prepared by thermal evaporation, *International Journal of Materials and Chemistry, 2012; 2*(4): 173-177.
[10] Ikhmayies, SJ, Ahmad-Bitar, RN. An Investigation of the bandgap and Urbach tail of vacuum-evaporated SnO_2 thin films. *Renewable Energy, 2013; 49*: 143-146.
[11] Sundqvist, J, Hårsta, A. Growth of SnO_2 thin films by ALD and CVD: A comparative study, In: *Proceedings of the sixteenth Int. CVD Conf. 2003, 1*: 511. Paris, France,
[12] Geraldo, V, De Andrade, SLV, De Morais, EA, Santilli, CV, Pulcinelli, SH. Sb Doping effect and oxygen adsorption in SnO_2 thin films deposited via sol-gel. *Mat. Res 2003; 6*(4): 451-456.
[13] Rakhshani, AE, Makdisi, Y, Ramazaniyan, HA. Electronic and optical properties of fluorine-doped tin oxide films. *J. Appl. Phys. 1998; 83*(2): 1049-1057.
[14] Ikhmayies, SJ. Production and Characterization of CdS/CdTe Thin Film Photovoltaic Solar Cells of Potential Industrial Use, *Ph.D. Thesis, University of Jordan*, Amman, Jordan, 2002.
[15] Gordillo, G, Moreno, LC, Cruz, WDL, Teheran, P. Preparation and characterization of SnO_2 thin films deposited by spray pyrolysis from $SnCl_2$ and $SnCl_4$ precursors. *Thin Solid Films 1994; 252*: 61-66.
[16] Shanthi, E, Banerjee, A, Dutta, V, Chopra, LK., Electrical and optical properties of tin oxide films doped with F and (Sb + F). *J. Appl. Phys.1982; 53*(3): 1615-1621.
[17] Ikhmayies, SJ. Optical parameters of Nanocrystalline SnO_2: F thin films prepared by the spray pyrolysis method. *JOM, 2019; 71*(4): 1507-1512.
[18] Ikhmayies, SJ. Properties of SnO_2: F thin films prepared by using HF or NH_4F after exposure to atmosphere. *Journal of Energy Systems, 2017; 1*(3): 120-128.
[19] Ikhmayies, SJ. The influence of annealing on the optical properties of spray-deposited SnO_2: F thin films. *International Journal of Hydrogen Energy, 2016; 41*(29): 12626-12633.
[20] Ikhmayies, SJ. Ahmad-Bitar, RN. Using I-V characteristics to investigate selected contacts for SnO_2: F thin films. *J. Semiconductors 2012; 33*(8): 083001-(1-6).
[21] Ikhmayies, SJ, Ahmad-Bitar, RN. An investigation of the bandgap and Urbach tail of spray-deposited SnO_2: F thin films. *Physica Scripta. 2011; 84*: 055801 (7 pp).
[22] Ikhmayies, SJ, Ahmad-Bitar, RN. Effect of the substrate temperature on the electrical and structural properties of spray-deposited SnO_2: F thin films. *Materials Science in Semiconductor Processing, 2009; 12*(3): 122-125.
[23] Ikhmayies, SJ, Ahmad-Bitar, RN. The effects of post-treatments on the photovoltaic properties of spray-deposited SnO_2: F thin films. *Applied Surface Science, 2008; 255*: 2627-2631.
[24] Ikhmayies, SJ, Ahmad-Bitar, RN. Effect of processing on the electrical properties of spray-deposited SnO_2: F thin films. *American Journal of Applied Sciences 2008; 5*(6): 672-677.
[25] Ikhmayies, SJ. A comparison between the properties of SnO_2: F thin films prepared by using different doping compounds: HF and NH_4F. In: Jiann-Yang Hwang, Chengguang Bai, John Carpenter, Shadia J Ikhmayies, Bowen Li, Sergio Neves Monteiro, Zhiwei Peng, Mingming Zhang edsitors. *Characterization of Minerals, Metals and Materials, 2013*, TMS (The Minerals, Metals and Materials Society), 2013.pp. 235-242.
[26] Metın, H, Esen, R. Photoconductivity studies on CdS films grown by chemical bath deposition technique. *Erciyes Üniversitesi Fen Bilimleri Enstitüsü Dergisi, 2003; 19*(1-2): 96-102.
[27] Sahay, PP, Nath, RK, Tewari, S. Optical properties of thermally evaporated CdS thin films. *Cryst. Res. Technol. 2008; 42*(3): 275-280.
[28] Ikhmayies, SJ. Tuning the properties of nanocrystalline CdS thin films. *JOM. 2014; 67*(1): 46-60.
[29] Ikhmayies, SJ. Characterization of nanocrystalline CdS thin films prepared by thermal evaporation. *International Journal of Materials and Chemistry, 2013; 3*(2): 28-33.
[30] Patidar, D, Sharma, Jain, RN, Sharma, TP, Saxena, NS. Optical properties of CdS sintered film. *Bull. Mater. Sci. 2006; 29*(1): 21-24.
[31] Ashour, A. Physical properties of spray pyrolysed CdS thin films. *Turk. J. Phys. 2003; 27*: 551-558.

[32] Ikhmayies, SJ. A study of the absorption Edge of CdS: In Thin Films**.** *International Journal of Materials and Chemistry 2018; 8*(1): 10-14. DOI: 10.5923/j.ijmc.20180801.02
[33] Ikhmayies, SJ. The influence of heat treatment on the optical parameters of spray-deposited CdS: In thin films, *JOM., 2017; 69* (2): 144-161.
[34] Ikhmayies, SJ, Ahmad-Bitar, RN. Dependence of the photoluminescence of CdS: In thin films on the excitation power of the laser, *Journal of Luminescence 2014; 149:* 240-244.
[35] Ikhmayies, SJ, Juwhari, HK. Ahmad-Bitar, RN. Nanocrystalline CdS: In thin films prepared by the spray-pyrolysis technique. *J. Luminouscence. 2013; 141*: 27-32.
[36] Ikhmayies, SJ, Ahmad-Bitar, RN. A study of the optical bandgap energy and Urbach tail of spray-deposited CdS: In thin films. *Journal of Materials Research and Technology*. *2013; 2*(3): 221-227.
[37] Ikhmayies, SJ, Ahmad-Bitar, RN. AC measurements of spray-deposited CdS: In thin films. *J. Cen. South Univ. 2012; 19:* 829-834.
[38] Ikhmayies, SJ, Ahmad-Bitar, RN. Interface photoluminescence of the SnO_2: F/CdS: In/CdTe thin film solar cells prepared partially by the spray pyrolysis technique. *J. Luminouscence. 2012; 132*: 502-506.
[39] Ikhmayies, SJ, Ahmad-Bitar, RN. The use of I-V characteristics for the investigation of selected contacts for spray-deposited CdS: In thin films. *Vacuum. 2011; 86*: 324-329.
[40] Ikhmayies, SJ, Ahmad-Bitar, RN. A comparison between the electrical and optical properties of CdS: In thin films for two doping ratios. *Jordan Journal of Mechanical and Industrial Engineering JJMIE. 2010; 4*(1): 111-116.
[41] Ikhmayies, SJ, Ahmad-Bitar, RN. The influence of the substrate temperature on the photovoltaic properties of spray-deposited CdS: In thin films. *Applied Surface Science*. *2010; 256*(11): 3541-3545.
[42] Ikhmayies, SJ, Ahmad-Bitar, RN. Effects of processing on the electrical and structural properties of spray-deposited CdS: In thin films. *Physica B: Condensed Matter*. *2009; 404* (16): 2419-2424.
[43] Ikhmayies, SJ, Ahmad-Bitar, RN. Effects of annealing in nitrogen atmosphere and HCl-etching on the photoluminescence spectra of spray-deposited CdS: In thin films. *Applied Surface Science*. *2009; 255*(20): 8470-8474.
[44] Ikhmayies, SJ, Ahmad-Bitar, RN. Effect of film thickness on the electrical and structural properties of CdS: In thin films. *American Journal of Applied Sciences. 2008; 5*(9): 1141-1143.
[45] Ikhmayies, SJ, Ahmad-Bitar, RN. Effect of film thickness on the electrical and structural properties of CdS: In thin films. *American Journal of Applied Sciences. 2008; 5*(9): 1141-1143.
[46] Weng, S, Cocivera, M. Cadmium sulphide prepared from cadmium oxide thin films. *Solar Energy Materials and solar cells 1995; 36*: 301-309.
[47] El Maliki, H, Berne`de, JC, Marsillac, S, Pinel, J, Castel, X, Pouzet, J. Study of the influence of annealing on the properties of CBD-CdS thin films. *Applied Surface Science. 2003; 205*: 65-79.
[48] Niles, DW, Rioux, D, Höchst, H. A photoemission investigation of the SnO_2/CdS interface: a front contact interface study of CdS/CdTe solar cells. *J.Appl.Phys.1993; 73*(9): 4586-4590.
[49] Krishnakumar, V, Ramamurthi, K, Klein, A, Jaegermann, W. Band alignment of differently treated TCO/CdS interfaces. *Thin Solid Films 2009; 517*: 2558-2561.
[50] Al Turkestani MK, Durose, K. Rectification in CdS/TCO bilayers. *Solar Energy Materials and Solar Cells. 2011; 95*(2): 491-496.
[51] Ikhmayies, SJ, Ahmad-Bitar, RN. Using HF rather than NH_4F as doping source for spray-deposited SnO_2: F thin films. *J. Cent. South Univ. 2012; 19*: 791-796.
[52] Lupan, O, Chow, L, Chai, G, Roldan, B, Naitabdi, A, Schulte, A, Heinrich, H. Nanofabrication and characterization of ZnO nanorod arrays and branched microrods by aqueous solution route and rapid thermal processing. *Materials Science and Engineering B, 2007; 145*: 57–66.
[53] Lattice Constants and Crystal Structures of some Semiconductors and Other Materials. Available at: https://7id.xray.aps.anl.gov/calculators/crystal_lattice_parameters.html. August 11, 2019.
[54] Dhere, RG, Moutinho, HR, Asher, S, Li, X, Ribelin, R, Gessert, T, Young, D. Characterization of SnO_2 films prepared using tin tetrachloride and tetra methyl tin precursors. In: *National Center for Photovoltaics Program Review Meeting Denver; September 8-11, 1998*, Colorado, USA.